Available online at www.sciencedirect.com
ScienceDirect
Earth and Planetary Science Letters 264 (2007) 284–298
EPSL
www.elsevier.com/locate/epsl

Satellite- and pollen-based quantitative woody cover reconstructions for northern Asia: Verification and application to late-Quaternary pollen data

Pavel Tarasov [a,*], John W. Williams [b], Andrei Andreev [c], Takeshi Nakagawa [d], Elena Bezrukova [e], Ulrike Herzschuh [c], Yaeko Igarashi [f], Stefanie Müller [a], Kirstin Werner [c], Zhuo Zheng [g]

[a] *Institute of Geological Sciences, Palaeontology Department, Free University, Malteserstr. 74-100, House D, Berlin, 12249, Germany*
[b] *Department of Geography, 550 North Park St., University of Wisconsin, Madison, WI 53706 USA*
[c] *Alfred-Wegener-Institute for Polar and Marine Research, Telegrafenberg A43, Potsdam, 14473, Germany*
[d] *Department of Geography, University of Newcastle upon Tyne, Newcastle upon Tyne, NE1 7RU, UK*
[e] *Institute of Geochemistry, Siberian Branch Russian Academy of Sciences, Favorsky Street 1a, Irkutsk, 664033, Russia*
[f] *Institute for Paleoenvironment of Northern Regions, Koyocho 3-7-5 Kitahiroshima, Hokkaido, 061-1134, Japan*
[g] *Department of Earth Sciences, Sun Yat-sen University, Guangzhou, 510275, China*

Received 31 May 2007; received in revised form 20 August 2007; accepted 2 October 2007
Available online 11 October 2007
Editor: H. Elderfield

Abstract

Accurate reconstruction of late-Quaternary vegetation cover is necessary for better understanding of past vegetation dynamics, the role of vegetation feedbacks in glacial–interglacial climate variations, and for validating vegetation and climate models. In this paper over 1700 surface-pollen spectra from the former Soviet Union, Mongolia, northern China, and northern Japan together with data from the Advanced Very High Resolution Radiometer (AVHRR) were used to calibrate modern-analogue method for quantitatively reconstructing past woody cover from fossil pollen data. The AVHRR-based estimates of woody cover percentages within a 21×21 km window around pollen sampling sites were attributed to the respective modern pollen spectra. Reconstructions of modern woody cover using the pollen data and best-modern-analogues (BMA) method matched well to the original AVHRR-based estimates, for both total woody cover ($r^2=0.77$) and its fractions, including broad-leaved ($r^2=0.66$), needle-leaved ($r^2=0.79$), deciduous ($r^2=0.60$) and evergreen ($r^2=0.76$) woody cover. Discrepancies in the pollen–AVHRR cross-validation may be caused by long-distance transport of arboreal pollen, patchy forest distributions, underrepresentation of *Larix* and *Populus* in pollen records, and errors in the AVHRR classification. The generally strong correlations encourage application of the modern-analogue approach for reconstructing late-Quaternary variations in vegetation cover from northern Asian fossil pollen records. At the last glacial maximum (LGM: ~21,000 cal yr BP), areas presently occupied by boreal forest were much more open, suggesting a reduction in total woody cover to below 20% at most modern forest sites. Pollen records from northern and central Siberia suggest a rather quick spread of tree and shrub vegetation after 15,000 cal yr BP, presumably in response to increased summer insolation.

* Corresponding author. Tel.: +49 30 83870280; fax: +49 30 83870745.
E-mail addresses: ptarasov@zedat.fu-berlin.de (P. Tarasov), jww@geography.wisc.edu (J.W. Williams), aandreev@awi-potsdam.de (A. Andreev), Takeshi.Nakagawa@NEWCASTLE.AC.UK (T. Nakagawa), bezrukova@igc.irk.ru (E. Bezrukova), Ulrike.Herzschuh@awi.de (U. Herzschuh), VZQ06055@nifty.ne.jp (Y. Igarashi), smueller@awi-potsdam.de (S. Müller), kirstinwerner@web.de (K. Werner), ee29@sysu.edu.cn (Z. Zheng).

doi:10.1016/j.epsl.2007.10.007

Woody cover histories are spatially variable in the modern forest-steppe, where tree growth is largely controlled by the ratio of annual actual over potential evapotranspiration which serves as an index of moisture availability. In northwestern Mongolia, woody cover percentages decreased between ~9000 and 5000 cal yr BP and again between 2000 and 1000 cal yr BP and may be linked to shifts in intensity of the Pacific monsoon. In contrast, pollen data from the Kazakhstan forest-steppe (where atmospheric precipitation is associated with the Atlantic westerly flow) suggest that woody cover density reached modern levels only during the last millennium.

Keywords: Northern Asia; pollen spectra; AVHRR; best-modern-analogue approach; woody cover; last glacial maximum; Holocene

1. Introduction

Pollen analyses and syntheses have significantly contributed to the objective reconstruction of late-Quaternary vegetation and climate, greatly facilitating research into past global changes and Earth system modelling (Wright et al., 1993; Prentice et al., 2000; Markgraf, 2001; Braconnot et al., 2004). Data from northern Asia are important to global-scale palaeoenvironmental studies because of the broad area covered, the well-defined gradients of modern vegetation and climate (Tarasov et al., 1999; Kageyama et al., 2001), and the critical role played by biophysical and biogeochemical vegetation feedbacks for amplifying high-latitude climate variability, both past and future (Foley et al., 1994; Ganopolski et al., 1998; Levis et al., 1999a,b; Betts, 2000). Over the past several decades the number of published late-Quaternary pollen records from northern Asia increased rapidly (Khotinskii, 1977; Velichko et al., 1984; Peterson, 1993; Gunin et al., 1999; Edwards et al., 2000; Tarasov et al., 2000). This increase in data quantity and quality enables continental-scale vegetation and climate reconstructions (Prentice et al., 2000; Tarasov et al., 1999, 2000; Edwards et al., 2000).

Transformation of pollen data into vegetation maps can be significantly improved by quantitative approaches (Prentice, 1985; Sugita, 1993). At stand to landscape scales, pollen-transport models have been successfully applied to reconstruct forest and cultural dynamics in northern Europe (Eklöf et al., 2004; Sugita, 2007a,b). The biomization method, which objectively assigns pollen spectra to major vegetation types, has been used for regional- to global-scale vegetation mapping (Prentice et al., 1992, 1996). In northern Eurasia, this method was successfully tested with extensive modern pollen datasets (Edwards et al., 2000; Tarasov et al., 1998) and applied to mid-Holocene and last glacial maximum (LGM) pollen spectra (Edwards et al., 2000; Tarasov et al., 2000). However, the biomization approach provides no quantitative information about vegetation composition or structure and can mask temporal variations in the internal structure and composition of biomes (Williams et al., 2004).

Recently a powerful technique to quantitatively reconstruct variations in late-Quaternary woody cover was applied to pollen spectra from North America (Williams, 2003; Williams and Jackson, 2003). The new method combined modern and fossil pollen records and satellite-based Advanced Very High Resolution Radiometer (AVHRR) data (DeFries et al., 1999b) with the best-modern-analogue (BMA) approach (Overpeck et al., 1985; Guiot, 1990), allowing fossil pollen samples attribution to the vegetation characteristics associated with their closest modern pollen analogues. An extensive surface-pollen dataset from North America was merged with AVHRR-based observations of woody cover and tests demonstrated that analogue-based approaches could reconstruct modern woody cover gradients (Williams, 2003; Williams and Jackson, 2003). The technique then was applied to fossil pollen records to map post-glacial changes in woody cover density (Williams, 2003). Although the BMA approach is frequently employed to infer past climates from fossil pollen assemblages (Overpeck et al., 1985; Guiot, 1990; Jackson and Williams, 2004; Tarasov et al., 2005), applications to quantitative vegetation reconstructions are relatively new.

In the present study, concentrated on northern Asia, we (1) created a reference dataset consisting of surface-pollen spectra and associated AVHRR-based estimates of woody cover density, (2) tested the accuracy of regional woody cover reconstructions using the BMA approach applied to the reference modern dataset, and (3) applied the method to selected LGM and Holocene pollen records. The quantitative reconstructions are then discussed together with conventional interpretations of these pollen records.

2. Study area: environments and vegetation

Northern Asia extends from the Ural Mountains to the Bering Strait (~5000 km) and from the Arctic coasts to central Mongolia (~3500 km), covering over 30% of Eurasia. Geographically, the border separating northern Asia from Europe is placed along the Ural Mountains (1895 m) and roughly corresponds to 60°E. The northern and eastern limits are the Arctic and Pacific Oceans. There is no obvious physiographic feature to anchor the southern limit; we place it at 47°N, which roughly corresponds to the southern limit of boreal conifer forests in Kazakhstan and Mongolia (Andreev and Tarasov, 2007).

West of 90°E, northern Asia is relatively flat and the vast West Siberian Lowland (<200 m) gradually transitions southwards to the hilly plains and low mountains of northern Kazakhstan (maximum elevation: 1566 m). East of 90°E, the topography is more complex. Lowlands occupy a 50 to 600 km-wide band along the Arctic Ocean. A number of plateaus and mountain ranges occupy Middle and East Siberia and Mongolia south of 70°N (Alpat'ev et al., 1976). Average altitudes generally exceed 1000 m and the highest peaks reach 4506 m in the Russian Altai and 4750 m in the central Kamchatka Peninsula.

Northern Asia is characterized by a continental climate with pronounced seasonality. In winter, weather is controlled by a strong Siberian anticyclone. Mean January temperatures are about −16 °C in the south and drop to −50 °C in central Yakutia (Alpat'ev et al., 1976; Leemans and Cramer, 1991). Mean July temperature varies by latitude from 20 °C to <4 °C. Over two-thirds of annual precipitation falls during the warm season, when the weather is controlled by the Atlantic westerly flow (in the west) and the Pacific monsoon (in the east). Annual precipitation is highest on the western slope of the Ural Mountains (up to 600 mm) and in the Far East region, which may receive >1000 mm. Precipitation decreases to <300 mm in the inland regions of Kazakhstan, central Yakutia and Mongolia (Alpat'ev et al., 1976; Leemans and Cramer, 1991).

The distribution of (simulated) potential natural vegetation in northern Asia (Fig. 1a) reveals a primarily latitudinal pattern, modified by altitude and slope aspect. Key driving variables include minimum winter temperatures and growing season length (names of bioclimatic variables, biomes, and plant functional types follow (Prentice et al., 1992)). We use BIOME1 to represent modern potential vegetation because it provides a simple, uniform and widely used vegetation classification (Prentice et al., 1992, 1996; Tarasov et al., 1998); the simulated biome distribution (Fig. 1a) is very similar to patterns established in regional botanical studies (Alpat'ev et al., 1976; Hou, 2001; Vostokova and Gunin, 2005). Cold desert with very sparse vegetation occurs on the Arctic islands and archipelagos. Tundra vegetation occupies lowlands north of the Polar Circle and upper-elevation regions. South of the tundra grow coniferous forests and woodlands, represented by cold-deciduous forest and taiga biomes. The cold-deciduous forest includes deciduous needle-leaved taxa such as *Larix* and broad-leaved taxa such as *Betula*, *Populus* and *Alnus*. Evergreen conifers such as *Abies*, *Picea* and *Pinus sibirica* dominate in the taiga. *Pinus sylvestris* occurs throughout northern Asian forests. Cool conifer forests, known also as southern taiga in the Russian botanical literature (Khotinskii, 1977; Alpat'ev et al., 1976), are dominated by conifers such as *Abies*, *Picea* and *Pinus* with a small admixture of cool-temperate arboreal taxa, e.g. *Tilia*, *Ulmus* and *Corylus*.

In the steppe, occupying vast areas of northern and central Kazakhstan, Mongolia and northern China, Poaceae, *Artemisia* and various mesophyllous herbs and shrubs dominate. The steppe is not completely unforested. In northern and central Kazakhstan, patchy forests mainly composed of *P. sylvestris*, *Betula* and *Populus* are associated with river valleys, fresh-water lakes, and low-elevation granite massifs (Alpat'ev et al., 1976). In the Mongolian forest-steppe, the dominant tree taxa are *Larix*, *Betula* and *Pinus* (Vostokova and Gunin, 2005). *Ulmus pumila* sometimes forms open floodplain forests in northeastern Mongolia and south of Lake Baikal (Tarasov et al., 2005; Vostokova and Gunin, 2005).

Desert vegetation occurs in innermost central Asia, where permanent vegetation cover is sparse and mainly represented by drought-tolerant herbaceous and shrubby taxa such as Chenopodiaceae, *Artemisia*, *Caragana*, *Ephedra*, *Nitraria*, *Zygophyllum*, *Peganum*, and *Tamarisk*. Trees, shrubs (mainly *Populus* and *Salix*), and more diverse herbaceous vegetation are found in riparian areas (Alpat'ev et al., 1976; Hou, 2001; Vostokova and Gunin, 2005).

3. Data and methods

3.1. AVHRR data

The modern estimates of woody cover (needle-leaved/broad-leaved and deciduous/evergreen) were produced from 1992 to 1993 AVHRR observations (DeFries et al., 1999b) in which each 1×1 km pixel was described as a percent mixture of several vegetation-cover categories defined by growth form (woody, herbaceous or bare ground), and woody vegetation was subdivided by leaf type (needleleaf or broadleaf) and leaf longevity (evergreen or deciduous). Woody coverage greater than 65% is

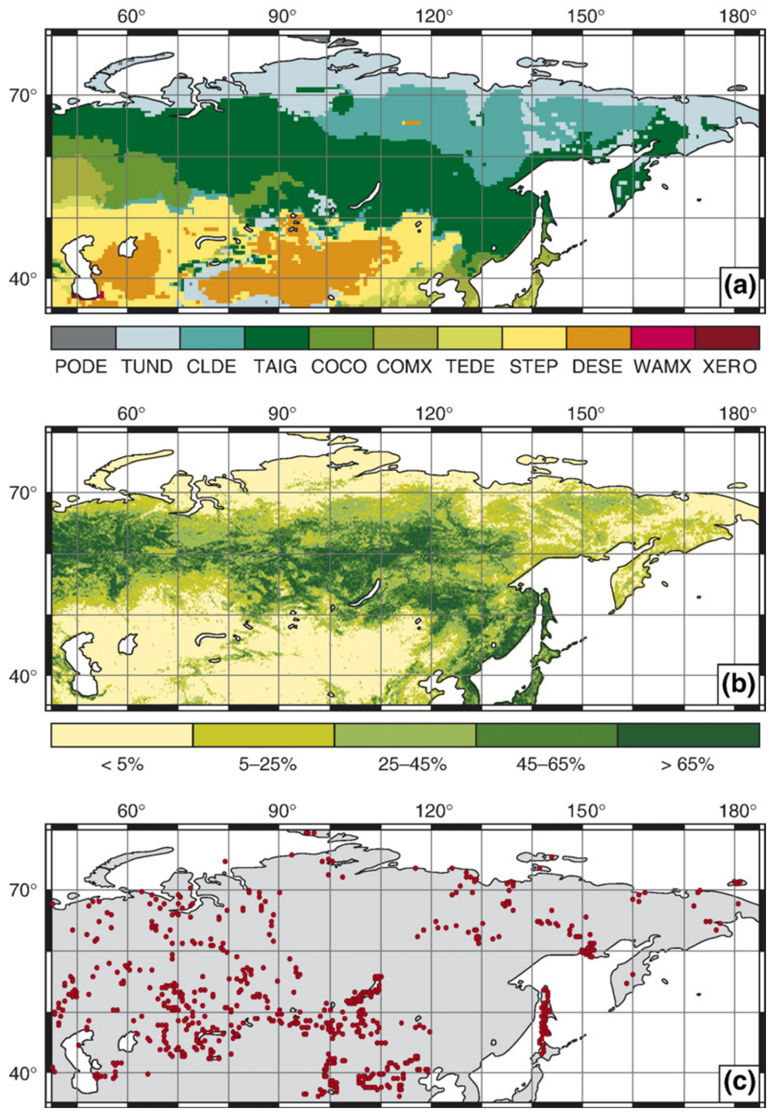

Fig. 1. Simplified maps showing (a) modern distribution of potential natural vegetation types (biomes); (b) AVHRR-derived values of woody cover percentages; (c) surface-pollen sampling sites used to verify the woody cover reconstruction method in northern Asia. Biomes are simulated using bioclimatic limits used in the BIOME1 model (Prentice et al., 1992) and modern climate data from Leemans and Cramer (Leemans and Cramer, 1991). In the legend PODE indicates polar desert, TUND — tundra, CLDE — cold-deciduous forest, TAIG — taiga, COCO — cool conifer forest, COMX — cool mixed forest, TEDE — temperate deciduous forest, STEP — steppe, including cool and warm grass/shrub, DESE — desert, including hot and cool desert/semi-desert, WAMX — warm mixed forest and XERO — xerophytic woods/scrub.

associated with the mid-latitudinal forest belt extending from the middle Ural Mountains towards Sakhalin and mainly corresponds to the taiga biome (Fig. 1a). Areas north and south of the taiga belt have moderate forest coverage (25–45%), suggesting greater landscape openness. Lower woody coverages (5–25%) mark transitional zones with forest-tundra and forest-steppe vegetation. Open vegetation dominates northern regions occupied by tundra and Arctic desert and southern regions occupied by steppe and desert (Fig. 1a,b).

AVHRR-based estimates of percent woody cover were assigned to each pollen surface sample by placing a 21 by 21 km window around each site and averaging the per-pixel AVHRR estimates of woody cover. The search window roughly approximates the pollen source area for the small lakes and mires typically studied by pollen analysts (Bradshaw and Webb, 1985); prior analyses suggest that pollen–AVHRR correlations are strongest for search windows from 20 by 20 km to 150 by 150 km (Williams and Jackson, 2003).

3.2. Surface-pollen spectra

A comprehensive compilation of surface-pollen spectra from northern Asia was stimulated by the BIOME 6000 project (Prentice et al., 2000) and continued afterwards. The dataset used here includes 1741 surface-pollen spectra and is largely based on prior regional compilations (Edwards et al., 2000; Tarasov et al., 2000). It includes 1173 pollen spectra from the former Soviet Union and Mongolia (Tarasov et al., 2005), 63 spectra from northwestern China (Herzschuh et al., 2004) and 505 spectra from unpublished sources compiled here from Siberia, Sakhalin, Hokkaido, and northern China. The sum of all terrestrial pollen taxa (Supplementary Table 1) was used to calculate relative pollen percentages.

3.3. Best-modern-analogue (BMA) approach

Details of the BMA approach and its palaeoecological applications are presented in many publications (Williams, 2003; Overpeck et al., 1985; Guiot, 1990; Jackson and Williams, 2004; Tarasov et al., 2005). We reconstructed five fractional cover types from the AVHRR dataset: broad-leaved, evergreen, deciduous, needle-leaved and total woody cover. The skill of the BMA approach was tested by comparing BMA-reconstructed values for the surface-pollen dataset (Fig. 1c) to the original AVHRR measurements. While in this testing mode, a modern sample was not allowed to find itself as the best analogue so that the BMA reconstructions are distinct from and can be assessed against the original woody cover values.

All BMA analyses used squared-chord distances (SCD) (Overpeck et al., 1985) as the index of dissimilarity between pollen spectra: two spectra were judged analogous if their SCD's were less than a threshold T. BMA estimates of woody cover are then calculated as weighted averages of the modern woody cover variables of the N best analogues, with the inverse SCD as weights. We experimented with T (0.1 to 0.6 at 0.1 intervals) and N (3 to 10), but found that these parameters influenced only slightly the generally good correlation coefficients between AVHRR observations and BMA reconstructions. However, lowering the threshold from 0.4 to 0.2 increased the number of no-analogue samples from ~0 to ~14% for the reference sites. We therefore set the threshold to 0.4 and kept the 8 best-modern-analogues. Analogue selection was not geographically constrained. BMA calculations were effected using Polygon 1.5 (http://dendro.naruto-u.ac.jp/~nakagawa/).

To assess method accuracy and precision, BMA-reconstructed modern woody coverages were linearly regressed against the original AVHRR woody coverages. We used the r^2 and root-mean squared error (RMSE) statistics to measure method precision, and the regression slope to assess accuracy. We used major-axis regression to estimate the slope, because ordinary least squares regression underestimates the true slope when there is uncertainty in the independent variable, as is the case for the AVHRR data (Williams et al., in press).

3.4. Fossil pollen record

After testing, we applied the BMA approach to a dataset of 26 published pollen records from northern Asia (listed in Supplementary Table 2) in order to reconstruct vegetation cover at the last glacial maximum (LGM: ~18,000 ^{14}C yr BP or ~21,000 cal yr BP). The LGM is characterized by global temperature, precipitation, atmospheric carbon dioxide concentrations and vegetation density substantially reduced below present values and is frequently chosen for palaeoenvironmental reconstructions and data-model comparisons (Wright et al., 1993; Prentice et al., 2000; Markgraf, 2001; Kageyama et al., 2001). The LGM pollen dataset was used previously to reconstruct biomes (Tarasov et al., 2000) and climates (Tarasov et al., 1999) and was updated here with several recently published records from northern Siberia (Andreev et al., 2003, 2002a,b, 2004).

To reconstruct late-glacial and Holocene vegetation dynamics, we selected four well-dated pollen records representing different modern vegetation regions: forest-tundra (Lama Lake, northern Siberia), cold-deciduous and taiga forests (Chabada Lake, central Siberia) and forest-steppes where plant-available moisture (the ratio of annual actual over potential evapotranspiration (Prentice et al., 1992)) is controlled by advection from the Atlantic Ocean (Pashennoe Lake, Kazakhstan) or the Asian monsoon (Hoton-Nur, Mongolia). For each record, the radiocarbon dates were calibrated to calendar years using CalPal ver.1.4 (http://www.calpal.de). Primary pollen data and supporting information are stored in the European and Global Pollen Databases.

Lama Lake (69°32′N; 90°12′E, 53 m) is located in an east–west oriented valley at the western margin of the Putorana Plateau (1701 m) in the south–west of Taymyr Peninsula (Andreev et al., 2004). The area is characterized by a continental climate with long severe winters and frost-free period of about 35 days. Mean January temperature is about −33 °C and mean July temperature reaches 10–14 °C. Annual precipitation ranges from 300 to 400 mm at low elevations to 600–800 mm on the western slopes of the Putorana Plateau. Modern vegetation cover in the region has a pronounced altitudinal gradient. Forests dominated by *Picea*, *Larix* and *Betula* grow in a narrow belt up to 200–400 m above sea level, being replaced by shrub and herb-dominated mountain tundra (Andreev et al., 2004). Steppe taxa have been also found on south-facing slopes. A 11.1 m PG1111 core was collected in the western part of the lake from a water depth of 52.2 m, ~3 km from the lake shore and over 30 radiocarbon dates were obtained (Andreev et al., 2004).

Chabada Lake (61°59′N, 129°22′E, 290 m) lies on the ancient erosion-accumulative plain of the Lena River in the Central Yakutian Depression (Tarasov et al., 1996). The region experiences an extreme continental climate with mean January temperature −42 °C and mean July temperature 18–19 °C. Annual precipitation is about 200–250 mm, but seasonal melt from permafrost supports primary (*Pinus*–*Larix*-dominated) and secondary (*Betula*–*Populus*-dominated) forest vegetation (Alpat'ev et al., 1976). Steppe and meadow-steppe plant communities occupy flood plains and dried out lake basins. Desert-like vegetation is associated with drift sand fields ('tukulans'). Six radiocarbon dates from 210±170 to 11,550±120 ^{14}C yr BP were obtained (Andreev et al., 1997).

Hoton-Nur (48°40′N, 88°18′E, 2083 m) lies in the Mongolian Altai, in northwestern Mongolia (Gunin et al., 1999). Mean January temperatures are between −25 and −20 °C and mean July temperature is about 15 °C. Annual precipitation is ~300 mm and falls mainly during the warm season. Steppe and meadow communities dominate nearby the lake (Gunin et al., 1999) and mountain tundra dominated by Cyperaceae and *Betula* shrubs occurs above 3000 m. *Picea* and *Larix* grow on mountain slopes south–west of the lake and in river valleys. Isolated stands and single trees of *Larix* and *P. sibirica* were registered north of the lake. The chronology is based on six radiocarbon dates from 2950±80 to 9070±150 ^{14}C yr BP and on the regional pollen stratigraphy (Gunin et al., 1999).

Pashennoe Lake (49°22′N, 75°24′E, 871 m) is situated in the lower elevations of the Karkarala Mountains (1099 m) in east-central Kazakhstan (Tarasov et al., 1996). Mean January temperature is about −16 °C, mean July temperature about 21 °C and annual precipitation about 250–300 mm. However, local climates around the lake are characterized by slightly milder summer and winter temperatures and higher precipitation (Tarasov and Kremenetskii, 1995). Hills and mountain slopes are covered by *P. sylvestris*-dominated open forests and woodlands, and *Betula*, *Populus* and *Salix* grow around the lake. Steppe vegetation dominates around a nearby granite mountain massif. The chronology is established by nine radiocarbon dates spanning from 750±110 to 11,710±90 ^{14}C yr BP (Tarasov et al., 1996; Tarasov and Kremenetskii, 1995).

4. Results and discussion

4.1. Test of the method with modern-day data

The pollen-based modern woody cover reconstructions and original AVHRR measurements match well (Figs. 2 and 3), providing satisfactory estimates of percent variance explained and RMSE for both total woody cover (r^2=0.77, RMSE=11.69) and the broad-leaved (r^2=0.66, RMSE=3.31), needle-leaved (r^2=0.79, RMSE=10.23), deciduous (r^2=0.60, RMSE=5.52) and evergreen (r^2=0.76, RMSE=10.51) woody cover fractions at the modern pollen sites. Accuracy is generally high but imperfect, with most slopes between 0.9 and 1.0: broad-leaved (slope=0.83, 95% Confidence Interval (CI): 0.80–0.87), needle-leaved (slope=0.92, 95%CI: 0.89–0.95), deciduous (slope=0.65, 95%CI: 0.62–0.69), evergreen (slope=0.93, 95%CI: 0.90–0.96) and total woody cover (slope=0.91, 95%CI: 0.88–0.94). Reasons for the notably low accuracy of the deciduous woody cover reconstructions are discussed below. Maps of pollen-based woody cover reconstructions and original AVHRR-based estimates (Fig. 3) also demonstrate spatially coherent patterns. Key patterns include:

1. Broad-leaved woody cover estimated from the AVHRR measurements (Fig. 3a) shows low values (<5%) for areas dominated by taiga, cold-deciduous forest, arctic–alpine tundra, steppe and desert (Fig. 1a). Slightly higher values (5–25%) occur in the mid-latitudinal forest belt (48–60°N) in Sakhalin Island and southern Siberia, where the natural forest vegetation includes high proportions of cold-tolerant broad-leaved taxa, including *Betula*, *Populus*, *Alnus* and *Salix*. Northeastern China and Hokkaido Island in Japan also have relatively high values of broad-leaved woody cover, where cool-mixed forests are dominated by a variety of boreal and temperate deciduous broad-leaved taxa. The pollen-based reconstruction (Fig. 3b) demonstrates very similar patterns. Several pollen samples from the high Arctic indicate higher values than shown by the AVHRR.
2. Needle-leaved woody cover estimates by the AVHRR (Fig. 3c) adequately captures the distribution of boreal

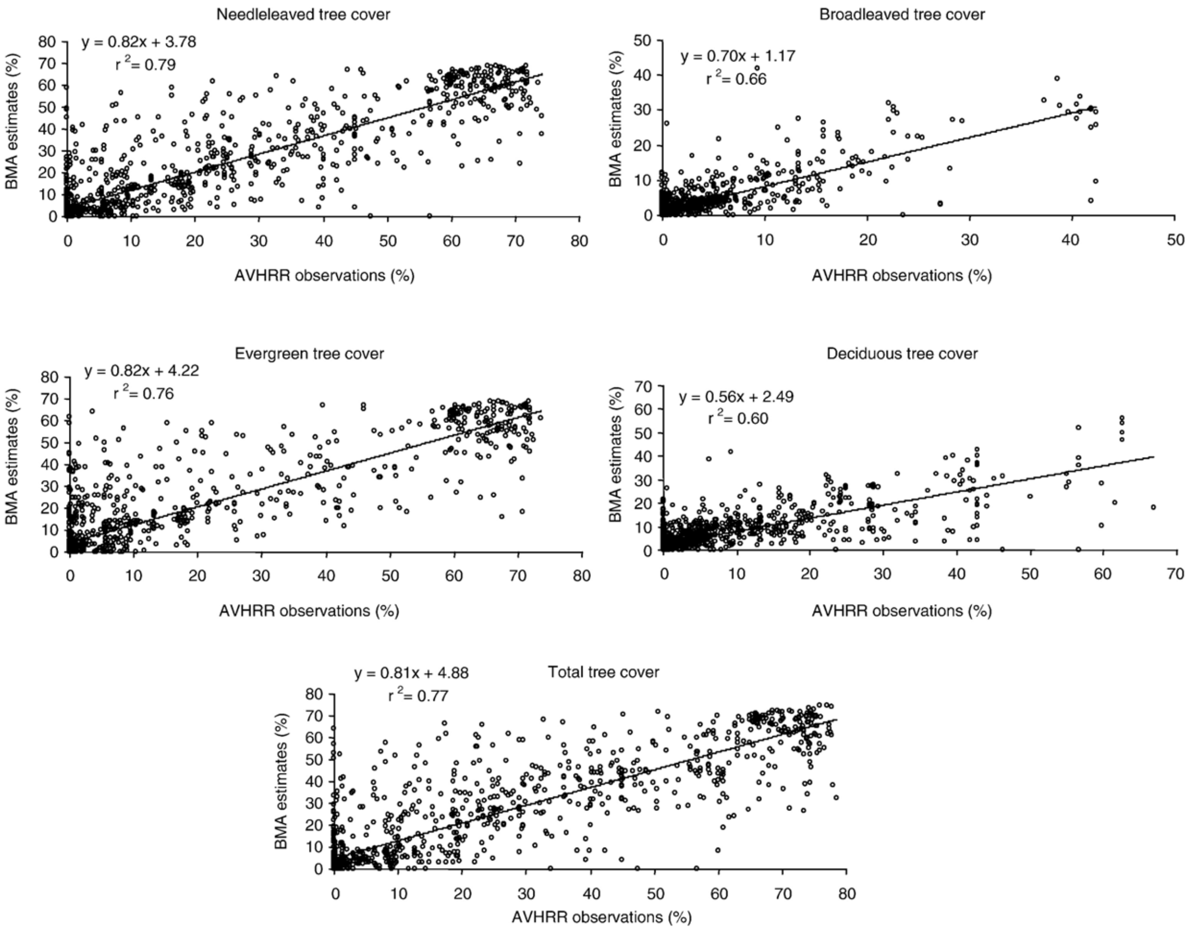

Fig. 2. Scatterplots comparing the original AVHRR-based observations of total woody cover and of woody cover fractions (needle-leaved, broad-leaved, evergreen, deciduous) with the analogue-based percent woody cover estimates for the modern pollen sites.

evergreen and deciduous conifer forests. The highest values occur in a latitudinal zone between 50 and 70°N from the north-central Urals through central Siberia to Sakhalin Island. Intermediate values are associated with the discontinuous *Pinus* and *Larix*-dominated forests found in Kazakhstan, Mongolia, northeastern China and Hokkaido. The pollen-based reconstructions (Fig. 3d) again show comparable results. However, in several cases needle-leaved woody cover estimates for Arctic islands with extremely sparse polar desert vegetation are distinctly higher than observations. Several pollen samples from the semi-desert and desert areas of central Asia also indicate higher values than shown by the original AVHRR estimates.

3. Deciduous woody coverages (Fig. 3e) are highest (>45%) in eastern Siberia, where cold-deciduous forests are dominated by *Larix*, and north of Lake Baikal, where *Larix* and *Betula*, are abundant. Pollen-based reconstructions demonstrate similar patterns (Fig. 3f), but they systematically underestimate deciduous woody cover (Fig. 2), particular for the eastern Siberian deciduous forests dominated by *Larix* and *Populus*.
4. Evergreen woody cover estimates (Fig. 3g) are highest (>45%) at sites located in the southern taiga from the Ural Mountains to Sakhalin Island. Moderate values are associated with the montane forests of central Asia, northeastern China and Hokkaido. Pollen-based reconstructions are (Fig. 3h) slightly higher than AVHRR estimates in the forest-tundra and cold-deciduous forest zone of northern Asia.

These reconstructions are consistent with prior biome reconstructions (Tarasov et al., 1998), which demonstrated that pollen-based vegetation reconstructions are less reliable for pollen samples from the hot deserts of central Asia and polar deserts of the Arctic islands with sparse or no permanent vegetation. In such regions, where local pollen production is extremely low, long-distant transport

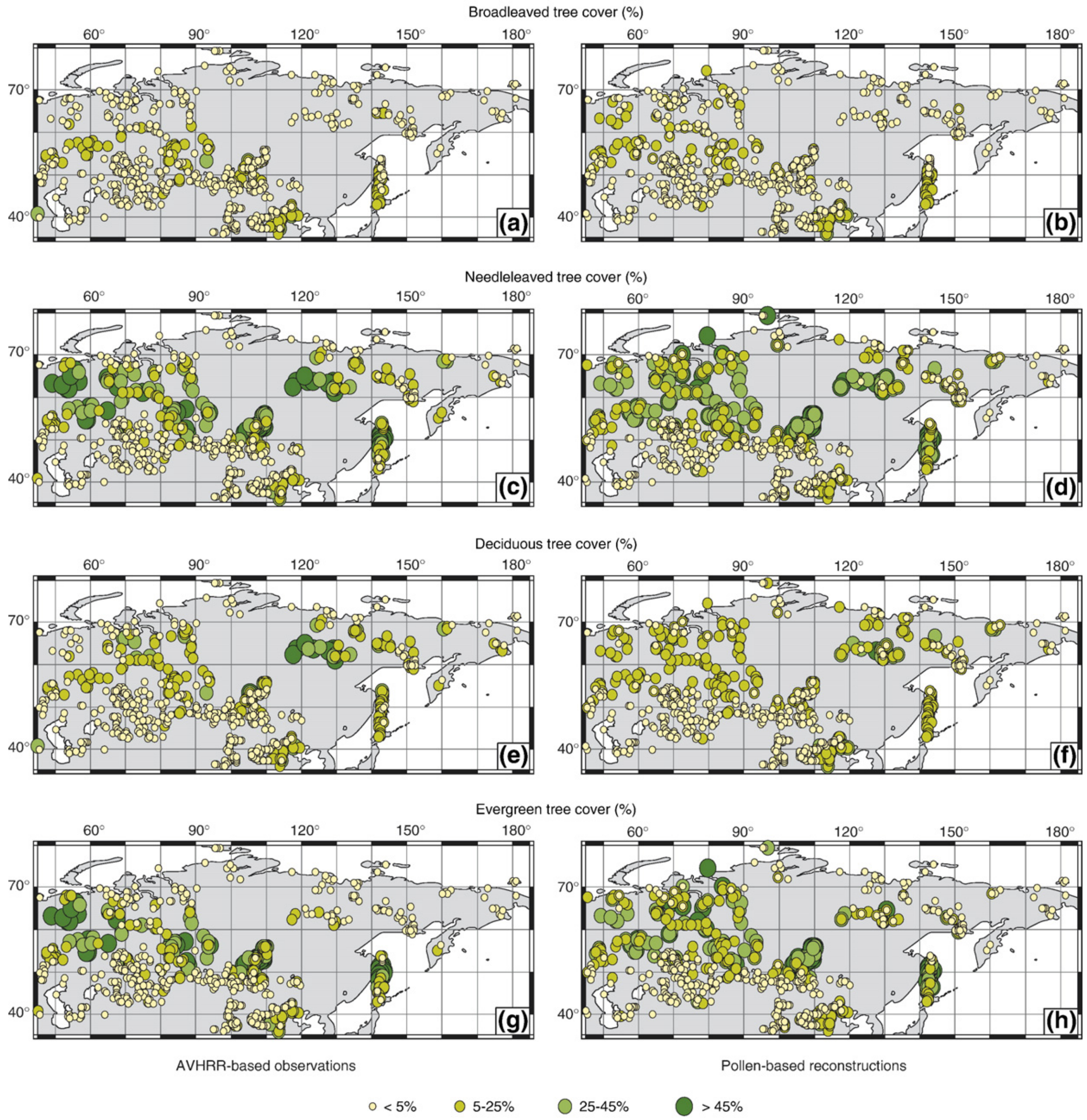

Fig. 3. Eurasian maps of present-day percent woody cover fractions generated using the original AVHRR-based observations and the pollen-based reconstructions for the modern pollen sites.

from adjacent forested areas substantially influences composition of pollen spectra, contributing a majority of identified pollen grains. The slightly higher-than-observed woody cover estimates in the forest-tundra and forest-steppe of north-central Asia may also be partially due to long-distance transport of arboreal pollen.

Discrepancies may also be caused by the differential sensitivity of the AVHRR and pollen sensors to local arboreal vegetation and/or spatial scale mismatches between the relevant source area of the pollen records and the 21 km × 21 km search window applied here to the AVHRR data. In particular, many pollen samples are located in patchy forests penetrating along north–south oriented river valleys deep into the tundra and steppe. This phenomenon is well known for the lower reaches of large Siberian rivers such as Lena, Yenisei and Ob' and the rivers crossing the central Asian steppes and deserts (Alpat'ev et al., 1976). Forest biomes are often reconstructed at pollen sites in northern Eurasia tundra where microclimates are favorable for local tree growth (Edwards et al., 2000; Tarasov et al., 1998).

Underestimated woody cover is especially noticeable for modern pollen sites where *Larix* and *Populus* trees dominate. Pollen from these taxa is badly distributed and poorly preserved during fossilization and thus is systematically underrepresented in pollen spectra (Peterson, 1993; Gunin et al., 1999; Edwards et al., 2000). The SCD metric used here is primarily sensitive to variations in the abundances of the most-common pollen types; for these areas, pollen-based vegetation reconstructions may be improved by metrics more sensitive to the presence of rare indicator taxa (Oswald et al., 2003).

Discrepancies between the AVHRR-estimated and pollen-reconstructed values of woody cover may also be due to inaccuracies in distinguishing needle-leaved and broad-leaved woody taxa using the AVHRR spectral data. The 10- to 30-day temporal resolution of composited data from the AVHRR sensor makes it well suited for capturing seasonal variations in phenology, and so the AVHRR estimates of deciduous versus evergreen woody taxa are relatively robust. The assignment of broad-leaved and needle-leaved designations onto the deciduous/evergreen woody data follows relatively simple rules (DeFries et al., 1999b), which may be in error when regional flora include substantial proportions of both broad-leaved and needle-leaved taxa within the deciduous and evergreen categories. This is a likely concern in Siberia, where deciduous needle-leaved taxa (*Larix*), deciduous broad-leaved taxa (*Populus*, *Betula*, *Alnus*) and evergreen needle-leaved taxa (*Picea*, *Pinus*) are regionally widespread.

Despite the above caveats, our generally successful results are consistent with prior work that also showed that 1) AVHRR-based methods successfully capture global vegetation patterns (DeFries et al., 1999a,b, 2000) and 2) analogue-based approaches can reproduce modern woody coverages with sufficient skill to justify paleovegetational reconstructions from fossil pollen data (Williams, 2003; Williams and Jackson, 2003). The r^2 values reported here are similar to those reported for North America ($r^2_{needle}=0.66$ and $r^2_{broad}=0.86$). The results thus encourage applying the BMA to reconstruct late-Quaternary variations in vegetation cover from northern Asian fossil pollen records.

4.2. LGM vegetation reconstructions

At the last glacial maximum, presently forested areas were much more open, such that total woody cover was below 20% at most of currently forested sites (Fig. 4). Woody cover anomalies (Modern - LGM) exceed 45% in the modern taiga (Fig. 4a). At two sites, however, reconstructed LGM woody cover was still moderately high, about 30–45% (Fig. 4b).

Prior qualitative (Grichuk, 1984; Frenzel et al., 1992; Petit-Maire et al., 2000) and quantitative (Tarasov et al., 1999, 2000; Edwards et al., 2000) reconstructions of LGM biomes agree with our finding that past vegetation structure was very different from today. However, prior interpretations have varied widely over the degree of sparseness of LGM vegetation. On the one hand, in the 'minimalistic' scenario (Ray and Adams, 2001) the vast area of northern Asia south and east of the ice sheet is shown as arctic and alpine desert with <2% of the ground covered by vascular plants. Steppe-tundra vegetation with ~50% vegetated cover is suggested for southern parts of the Far East and West Siberian Plain. On the other hand, Crowley (Crowley, 1995) reconstructs a conifer forest belt across western and central Siberia within 55–60°N during the LGM. LGM vegetation maps compiled by Grichuk (Grichuk, 1984; Frenzel et al., 1992) also show boreal conifer and deciduous trees in southern and central Siberia between 55 and 65°N, suggesting many scattered refugia from which tree vegetation could quickly spread as climates warmed. Brubaker et al. (2005), re-analyzing extensive pollen datasets from northeastern Siberia and Alaska, also concluded that small populations of boreal trees and shrubs, including *Larix*, *Pinus*, *Alnus* and *Betula*, were capable of surviving long periods of harsh climate and expanded as climates ameliorated. This interpretation is consistent with the Siberian Paleolithic radiocarbon database (Vasil'ev et al., 2002), which provides numerous conventional and AMS dates on wood and charcoal from 16 archaeological sites (Supplementary Table 3) in southern Siberia and Russian Far East (Fig. 4a), suggesting presence of woody plants and human populations in these regions even during the LGM. Prior biome reconstructions also indicate a mosaic pattern of the LGM vegetation in the mid-latitudes and suggest that the boreal forest belt was much reduced and likely discontinuous (Edwards et al., 2000; Tarasov et al., 2000). Our quantitative woody cover reconstructions support this more 'moderate' scenario.

This scenario of moderate reductions in woody cover at the LGM is also consistent with results from North America (Williams, 2003), demonstrating that during the LGM, woody cover was substantially reduced below present values, but open conifer woodlands and parklands existed south of Laurentide ice sheet in eastern North America. The reconstructed vegetation patterns were explained by the combined effect of colder- and drier-than-present LGM climates and reduced CO_2 concentrations. Similar factors likely influenced vegetation cover in northern Asia

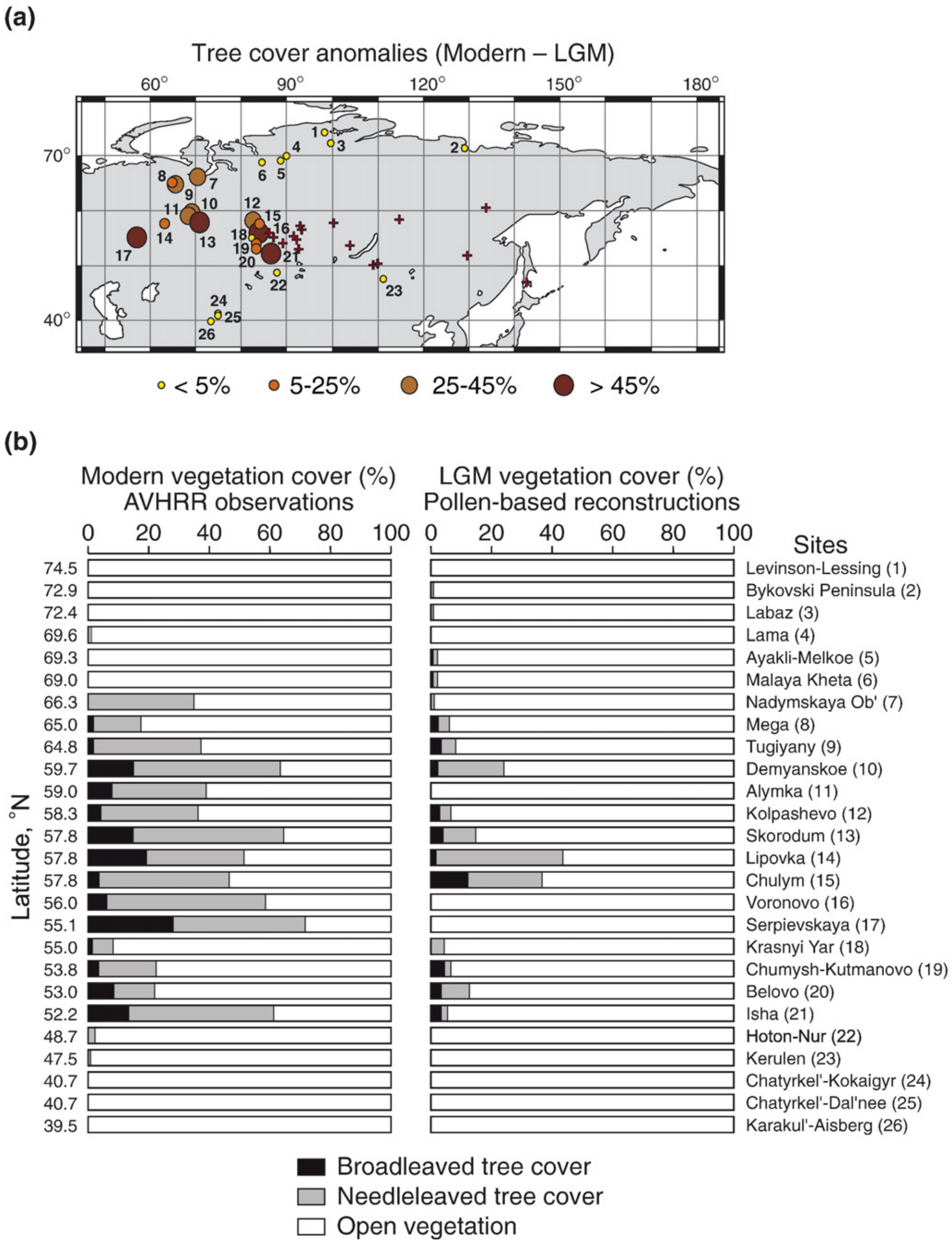

Fig. 4. LGM woody cover reconstructions for northern Asia derived from the LGM pollen records using the best-modern-analogue approach and extensive surface-pollen/AVHRR dataset from northern Eurasia. (a) The spatial distribution of the reconstructed anomalies. Larger-diameter circles correspond to greater modern afforestation of the study sites. Crosses show locations of radiocarbon-dated wood and charcoal material from archaeological sites in southern Siberia and Russian Far East (Vasil'ev et al., 2002). (b) LGM vegetation-cover reconstructions (right column) versus modern AVHRR-based estimates (left column) for the 26 sites with the LGM pollen data from northern Asia.

(Tarasov et al., 1999; Kageyama et al., 2001). Both reconstructed (Tarasov et al., 1999) and simulated (Kageyama et al., 2001) LGM climates allow growth of boreal needle-leaved and broad-leaved trees in southern Siberia, in agreement with available palaeobotanical evidences.

4.3. Application to the late-glacial and Holocene pollen records

Woody cover histories based on pollen records from northern (Fig. 5a) and central Siberia (Fig. 5b) suggest a quick expansion of trees and shrubs after 12,000 cal yr BP.

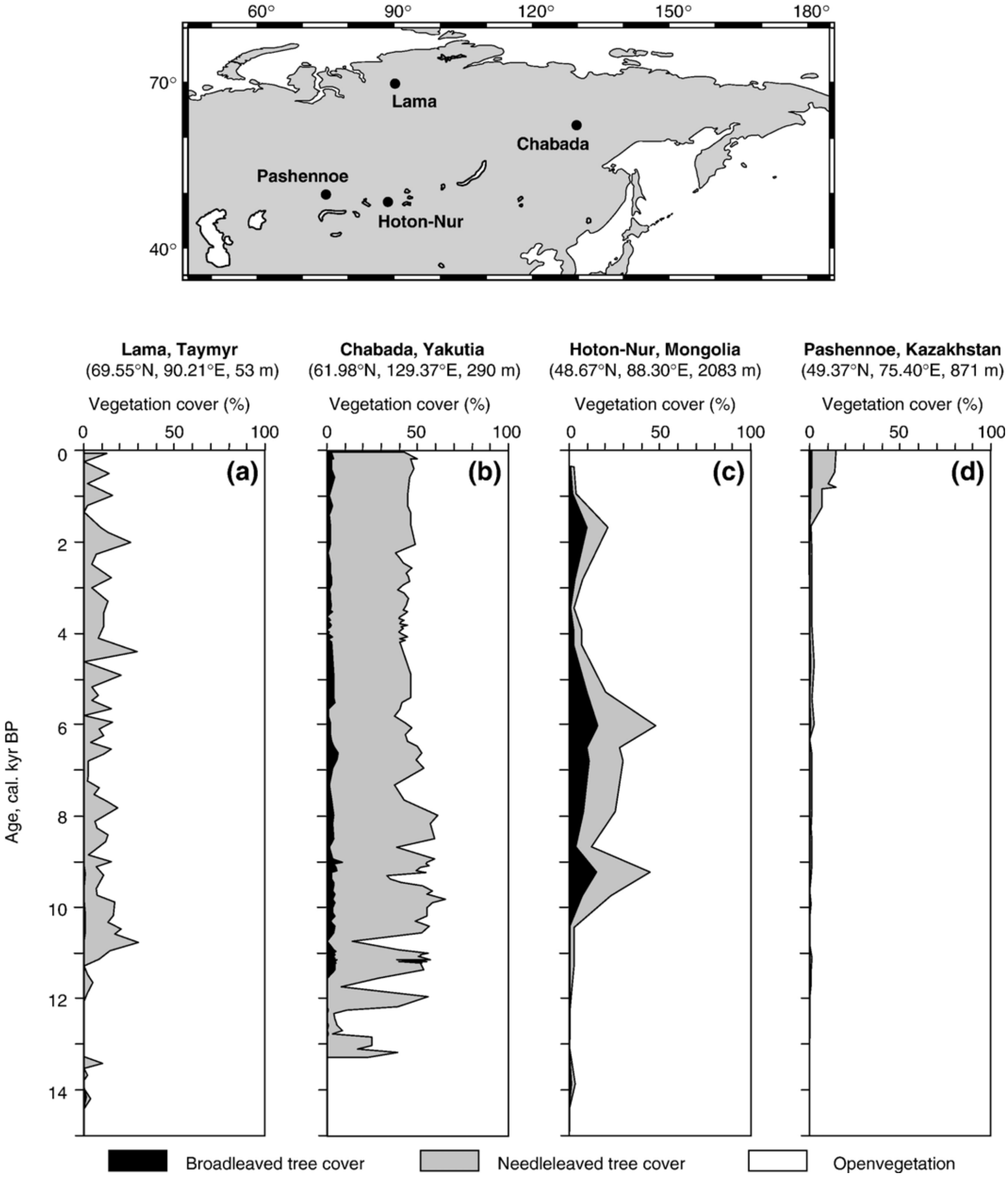

Fig. 5. Post-glacial changes in vegetation cover derived from four pollen records (see map for locations) representing different geographical and climatic regions of northern Asia.

These reconstructions agree well with the qualitative interpretations in the original publications (Gunin et al., 1999; Andreev et al., 2004, 1997; Tarasov and Kremenetskii, 1995) and with regional vegetation and biome reconstructions (Khotinskii, 1977; Velichko et al., 1984; Tarasov et al., 1998; Andreev and Tarasov, 2007). At Lake Lama, tree and shrub pollen produced by *Larix*, *Pinus*, *Picea*, *Salix*, *Betula* and *Alnus* are registered in small quantities (1–15%) after the LGM with a distinct peak associated with post-glacial (Allerød) warming (Andreev et al., 2004). The late-glacial/Holocene transition, dated to ~11,500 cal yr BP, is characterized by increased arboreal pollen (*Betula* sect. *Albae*, *Larix* and *Picea*) and decreased pollen abundances of arctic herbs and dwarf-shrubs. Qualitative interpretations of the pollen spectra and pollen-based biome reconstructions (Andreev et al., 2004) suggest a transition from tundra to forest-tundra (or woodland) vegetation with the onset of the Holocene, consistent with our woody cover reconstruction (Fig. 5a). Needle-leaved woody cover was maximal during the early Holocene, ~11,000–8000 cal yr BP. This corroborates with a compilation of radiocarbon-dated tree macrofossil data (Kremenetski et al., 1998) that indicates a more northern than present position of *Larix* in Siberia during the early Holocene. An extensive search and dating of tree macrofossils from the Eurasian Arctic (MacDonald et al., 2000) provides further proof that after an initial spread ~11,500 cal yr BP, boreal forest across northern Asia advanced to near the current Arctic coastline between ~10,000 and 8000 cal yr BP and retreated to its present position between ~4500 and 3000 cal yr BP. The northward expansion of forest was attributed to a combination of high summer insolation, ice sheet retreat, low sea-ice coverage and greater continentality associated with lower-than-present sea level (MacDonald et al., 2000).

The Lake Chabada pollen record demonstrates a locally quick afforestation during the late-glacial time (Andreev et al., 1997), synchronous with other pollen records from central Yakutia, and likely due to the Allerød warming (Andreev and Tarasov, 2007). After a brief phase of low woody cover between 13,000 and 12,000 cal yr BP associated with a Younger Dryas-like cooling event, forests dominated by *Betula* and *Larix* expanded into regions previously occupied by herbaceous and dwarf shrub vegetation. *P. sylvestris* was present in the region since the early Holocene, but became much more abundant after ~7000 cal yr BP, likely benefiting from a degradation of the permafrost layer (Andreev and Tarasov, 2007).

Woody cover histories are spatially variable in the modern forest-steppe (Fig. 5c–d), where tree growth is largely controlled by moisture availability. At Hoton-Nur in northwestern Mongolia (Fig. 5c), woody coverages were highest between 10,000 and 5000 cal yr BP and decreased to present levels around 4000 cal yr BP. The late-glacial and early Holocene pollen spectra were dominated by non-arboreal taxa, such as *Artemisia*, Chenopodiaceae and Poaceae, which were gradually replaced by high percentages of arboreal conifer and deciduous taxa, such as *Picea*, *Pinus*, *Larix* and *Betula*, between 10,000 and 5000 cal yr BP (Gunin et al., 1999; Andreev and Tarasov, 2007). This change in pollen composition is interpreted to indicate a vegetation change from dry steppe to woodland with patches of boreal taiga and cold-deciduous forests, supported by noticeably wetter conditions than those prevailing at present. This interpretation is consistent with regional sedimentary and diatom records, which suggest higher-than-present lake levels and fresh-water environments (Tarasov et al., 1996). The changes in pollen abundances, woody cover and climate in northwestern Mongolia are coherent with a Holocene monsoon precipitation reconstruction derived from Chinese stalagmites (Wang et al., 2005), which shows a strong summer monsoon at 9000 cal yr BP and decreased precipitation during the middle to late Holocene with the minimum between 1000 and 500 cal yr BP. Moreover, the record from Dongge Cave is punctuated by eight centennial-scale weak monsoon events centered at ~8300, 7200, 6300, 5500, 4400, 2700, 1600 and 500 cal yr BP (Wang et al., 2005). The resolution and dating quality of the Hoton-Nur pollen record does not permit close comparison with the isotope-inferred precipitation records from China. However, decreases in arboreal pollen percentages (Gunin et al., 1999; Andreev and Tarasov, 2007) and reconstructed woody cover (Fig. 5c) are observed about 8300, 6300, 5500–2700, and after 1500 cal yr BP, suggesting a linkage between the Pacific Ocean monsoon and forest extent in northwestern Mongolia.

In contrast to the other records reviewed here (Fig. 5a–c), woody cover density around Lake Pashennoe, situated close to the southern tree line in central Kazakhstan (Fig. 5d), apparently reached modern levels only during the last millennium. The Lake Pashennoe pollen diagram (Tarasov and Kremenetskii, 1995) contains high percentages of steppe- and desert-associated herbaceous taxa, such as *Artemisia*, Chenopodiaceae and Poaceae, throughout the late-glacial period and early to middle Holocene. Since ~6000 cal yr BP, arboreal taxa, such as *Betula* sect. *Albae* and *P. sylvestris* are more abundant, reflecting gradual spread of outlier stands of pines in northern and eastern Kazakhstan (Andreev and Tarasov, 2007; Tarasov and Kremenetskii, 1995). As at Hoton-Nur, the reconstructed spread of boreal forests in Kazakhstan indicates increased soil moisture availability. This increase, however, is not related to changes in Pacific circulation, because regional summer and partly winter circulation and precipitation patterns currently are controlled by 1) the movement of Atlantic air masses driven by shifts in westerly flow, 2) the efficiency of hydrological recycling during the several precipitation/evaporation cycles experienced during advective water transport to the Asian interior, and 3) local to regional atmospheric processes (Alpat'ev et al., 1976). Various climate proxies from western and northern Europe suggest that late-Holocene (~4500 cal yr BP – present) climates were cooler and wetter than present (Barber et al., 2004; Snowball et al., 2004). This trend from warm and dry middle-Holocene climates to cool and wet late-Holocene environments likely is driven by declining summer insolation and associated cooling of Arctic waters and reduced summer evaporation (Snowball et al., 2004). Orbitally forced PMIP climate simulations (Braconnot et al., 2004) for 6000 cal yr BP indicate increased temperature seasonality over the northern continents with summer temperatures >2 °C higher-than-present between

40 and 50°N. In Eurasia this summer thermal maximum intensified land–ocean temperature contrasts and enhanced monsoonal moisture advection (Braconnot et al., 2004). However, in Kazakhstan and southwestern Siberia, situated outside of the monsoon influence, warmer-than present summer temperatures would increase evaporation losses, thus lowering moisture availability.

5. Conclusion

This paper is the first attempt to quantify late-Quaternary woody cover densities in northern Asia and one of the first attempts to combine modern pollen datasets with remotely sensed vegetational indices. Tests show analogue-based approaches can reproduce present-day characteristics of woody cover in northern Asia with a reasonably high accuracy and precision. Application of the best-modern-analogue technique to published LGM and post-glacial pollen records from northern Asia suggest moderate reductions in forest cover at the LGM and spatially variable post-glacial vegetation histories that are consistent with and complementary to prior biome and quantitative climate reconstructions. There is great potential for hemispheric-scale reconstruction of late-Quaternary woody cover changes, using pollen records stored in the European, Global and Chinese pollen databases.

Acknowledgements

We acknowledge the EPD and GPD efforts to collect and assemble the pollen data used here and all palynologists who contributed their surface-pollen data to these databases and the IGBP-PAGES-sponsored BIOME6000 project. We thank N. Gorban' for cartographic assistance. The work of Andreev and Müller was financed by the German Research Foundation (DFG) project RI 809/17-1 and Williams' contribution was supported by the Earth System History Program of the National Science Foundation (ATM-0507999).

Appendix A. Supplementary data

Supplementary data associated with this article can be found, in the online version, at doi:10.1016/j.epsl.2007.10.007.

References

Alpat'ev, A.M., Arkhangel'skii, A.M., Podoplelov, N.Y., Stepanov, A.Y., 1976. Fizicheskaya geografiya SSSR (Aziatskaya chast'). Vysshaya Shkola, Moscow. 359 pp.

Andreev, A.A., Tarasov, P.E., 2007. Pollen records, postglacial: Northern Asia. In: Elias, S.A. (Ed.), Encyclopedia of Quaternary Science, vol. 4. Elsevier, Amsterdam, pp. 2721–2729.

Andreev, A.A., Klimanov, V.A., Sulerzhitskii, L.D., 1997. Younger Dryas pollen records from central and southern Yakutia. Quat. Int. 41/42, 111–117.

Andreev, A.A., Schirrmeister, L., Siegert, Ch., Bobrov, A.A., Demske, D., Seiffert, M., Hubberten, H.-W., 2002a. Paleoenvironmental changes in northeastern Siberia during the Upper Quaternary - evidence from pollen records of the Bykovsky Peninsula. Polarforschung 70, 13–25.

Andreev, A.A., Siegert, C., Klimanov, V.A., Dereviagin, A.Yu., Shilova, G.N., Melles, M., 2002b. Late Pleistocene and Holocene vegetation and climate changes in the Taymyr lowland, Northern Siberia reconstructed from pollen records. Quat. Res. 57, 138–150.

Andreev, A.A., Tarasov, P.E., Siegert, Ch., Ebel, T., Klimanov, V.A., Bobrov, A.A., Melles, M., Dereviagin, A.Yu., Hubberten, H.-W., 2003. Vegetation and climate changes on the northern Taymyr, Russia during the Upper Pleistocene and Holocene reconstructed from pollen records. Boreas 32 (3), 484–505.

Andreev, A.A., Klimanov, V.A., Siegert, C., Melles, M., Lisitsina, O.M., Hubberten, H.-W., 2004. Vegetation and climate changes around the Lama Lake, Taymyr Peninsula during the Late Pleistocene and Holocene reconstructed from pollen records. Quat. Int. 122, 69–84.

Barber, K., Zolitschka, B., Tarasov, P., Lotter, A.F., 2004. Atlantic to Urals — the Holocene climatic record of mid-latitude Europe. In: Battarbee, R.W., Gasse, F., Stickley, C.E. (Eds.), Past Climate Variability through Europe and Africa. Developments in Paleoenvironmental Research, vol. 6. Springer, Dordrecht, pp. 417–442.

Betts, R.A., 2000. Offset of the potential carbon sink from boreal forestation by decreases in surface albedo. Nature 408, 187–190.

Braconnot, P., Harrison, S.P., Joussaume, S., Hewitt, C.D., Kitoh, A., Kutzbach, J.E., Liu, Z., Otto-Bleisner, B., Syktus, J., Weber, S.L., 2004. Evaluation of PMIP coupled ocean-atmosphere simulations of the mid-Holocene. In: Battarbee, R.W., Gasse, F., Stickley, C.E. (Eds.), Past Climate Variability through Europe and Africa. Developments in Paleoenvironmental Research, vol. 6. Springer, Dordrecht, pp. 515–550.

Bradshaw, R.H.W., Webb III, T., 1985. Relationships between contemporary pollen and vegetation data from Wisconsin and Michigan, USA. Ecology 66, 721–737.

Brubaker, L.B., Anderson, P.M., Edwards, M.E., Lozhkin, A.V., 2005. Beringia as a glacial refugium for boreal trees and shrubs: new perspectives from mapped pollen data. J. Biogeogr. 32 (5), 833–848.

Crowley, T.J., 1995. Ice-age terrestrial carbon changes revisited. Glob. Biogeochem. Cycles 9, 377–389.

DeFries, R., Field, C., Fung, I., Collatz, G.J., Bounoua, L., 1999a. Combined satellite data and biogeochemical models to estimate global effects of human-induced land cover change on carbon emissions and primary productivity. Glob. Biogeochem. Cycles 13, 803–815.

DeFries, R.S., Townshend, J.R.G., Hansen, M.C., 1999b. Continuous fields of vegetation characteristics at the global scale at 1-km resolution. J. Geophys. Res. 104, 16911–16923.

DeFries, R.S., Hansen, M.C., Townshend, J.R.G., 2000. Global continuous fields of vegetation characteristics: a linear mixture model applied to multi-year 8 km AVHRR data. Int. J. Remote Sens. 21, 1389–1414.

Edwards, M.E., Anderson, P.M., Brubaker, L.B., Ager, T.A., Andreev, A.A., Bigelow, N.H., Cwynar, L.C., Eisner, W.R., Harrison, S.P., Hu, F.-S., Jolly, D., Lozhkin, A.V., MacDonald, G.M., Mock, C.J.,

Ritchie, J.C., Sher, A.V., Spear, R.W., Williams, J.W., Yu, G., 2000. Pollen-based biomes for Beringia 18,000, 6000 and 0 ^{14}C yr BP. J. Biogeogr. 27 (3), 521–554.
Eklöf, M., Broström, A., Gaillard, M.-J., Pilesjö, P., 2004. OPEN-LAND3: a computer program to estimate plant abundance around pollen sampling sites from vegetation maps: a necessary step for calculation of pollen productivity estimates. Rev. Palaeobot. Palynol. 132 (1–2), 67–77.
Foley, J.A., Kutzbach, J.E., Coe, M.T., Levis, S., 1994. Feedbacks between climate and boreal forests during the Holocene epoch. Nature 371, 52–54.
Frenzel, B., Pecsi, B., Velichko, A.A., 1992. Atlas of palaeoclimates and palaeoenvironments of the Northern Hemisphere. INQUA/ Hungarian Academy of Sciences, Budapest.
Ganopolski, A., Kubatzki, C., Claussen, M., Brovkin, V., Petoukhov, V., 1998. The influence of vegetation–atmosphere–ocean interaction on climate during the mid-Holocene. Science 280, 1916–1919.
Grichuk, V.P., 1984. Late Pleistocene vegetation history. In: Velichko, A.A., WrightJr. Jr., H.E., Barnosky, C.W. (Eds.), Late Quaternary environments of the Soviet Union. University of Minnesota Press, Minneapolis, MN, pp. 155–178.
Guiot, J., 1990. Methodology of the last climatic cycle reconstruction from pollen data. Palaeogeogr. Palaeoclimatol. Palaeoecol. 80, 49–69.
Gunin, P.D., Vostokova, E.A., Dorofeyuk, N.I., Tarasov, P.E., Black, C.C. (Eds.), 1999. Vegetation dynamics of Mongolia. Geobotany, vol. 26. Kluwer Academic Publishers, Dordrecht. 238 pp.
Herzschuh, U., Tarasov, P., Wünnemann, B., Hartmann, K., 2004. Holocene vegetation and climate of the Alashan Plateau, NW China, reconstructed from pollen data. Palaeogeogr. Palaeoclimatol. Palaeoecol. 211 (1–2), 1–17.
Hou, H. (Ed.), 2001. Vegetation atlas of China. Science Press China, Beijing.
Jackson, S.T., Williams, J.W., 2004. Modern analogs in Quaternary paleoecology: here today, gone yesterday, gone tomorrow? Annu. Rev. Earth Planet. Sci. 32, 495–537.
Kageyama, M., Peyron, O., Pinot, S., Tarasov, P., Guiot, J., Joussaume, S., Ramstein, G., 2001. PMIP participating groups, the Last Glacial Maximum climate over Europe and western Siberia: a PMIP comparison between models and data. Clim. Dyn. 17 (1), 23–43.
Khotinskii, N.A., 1977. Golotsen Severnoi Evrazii. Nauka, Moscow. 199 pp.
Kremenetski, C.V., Sulerzhitsky, L.D., Hantemirov, R., 1998. Holocene history of the northern range limits of some trees and shrubs in Russia. Arct. Alp. Res. 30 (4), 317–333.
Leemans, R., Cramer, W., 1991. The IIASA database for mean monthly values of temperature, precipitation and cloudiness of a global terrestrial grid. International Institute for Applied Systems Analysis (IIASA), RR-91-18.
Levis, S., Foley, J.A., Pollard, D., 1999a. Potential high-latitude vegetation feedbacks on CO_2-induced climate change. Geophys. Res. Lett. 26, 747–750.
Levis, S., Foley, J., Pollard, D., 1999b. CO_2, climate, and vegetation feedbacks at the Last Glacial Maximum. J. Geophys. Res. 104 (D24), 31191–31198.
MacDonald, G.M., Velichko, A.A., Kremenetski, C.V., Borisova, O.K., Goleva, A.A., Andreev, A.A., Cwynar, L.C., Riding, R.T., Forman, S.L., Edwards, T.W.D., Aravena, R., Hammarlund, D., Szeicz, J.M., Gattaulin, V.N., 2000. Holocene treeline history and climate change across northern Eurasia. Quat. Res. 53, 302–311.
Markgraf, V. (Ed.), 2001. Interhemispheric Climate Linkage. Academic Press, San Diego, CA. 454 pp.
Oswald, W.W., Brubaker, L.B., Hu, F.S., Gavin, D.G., 2003. Pollen-vegetation calibration for tundra communities in the Arctic Foothills, northern Alaska. J. Ecol. 91, 1022–1033.
Overpeck, J.T., Webb III, T., Prentice, I.C., 1985. Quantitative interpretation of fossil pollen spectra: dissimilarity coefficients and the method of modern analogs. Quat. Res. 23, 87–108.
Peterson, G.M., 1993. Vegetational and climatic history of the western former Soviet Union. In: Wright Jr., H.E., Kutzbach, J.E., Webb III, T., Ruddiman, W.F., Street-Perrott, F.A., Bartlein, P.J. (Eds.), Global climates since the last glacial maximum. University of Minnesota Press, Minneapolis, pp. 169–193.
Petit-Maire, N., Bouysse, P., de Beaulieu, J.-L., Boulton, G., Guo, Z., Iriondo, M., Kershaw, P., Lisitsyna, O., Partridge, T., Pflaumann, U., Schulz, H., Soons, J., van Vliet-Lanoë, B., 2000. Geological records of the recent past, a key to the near future world environments. Episodes 23 (4), 230–246.
Prentice, I.C., 1985. Pollen representation, source area, and basin size: toward a unified theory of pollen analysis. Quat. Res. 23, 76–86.
Prentice, I., Cramer, W., Harrison, S.P., Leemans, R., Monserud, R.A., Solomon, A.M., 1992. A global biome model based on plant physiology and dominance, soil properties and climate. J. Biogeogr. 19, 117–134.
Prentice, I.C., Guiot, J., Huntley, B., Jolly, D., Cheddadi, R., 1996. Reconstructing biomes from palaecological data: a general method and its application to European pollen data at 0 and 6 ka. Clim. Dyn. 12, 185–194.
Prentice, I.C., Jolly, D., BIOME 6000 participants, 2000. Mid-Holocene and glacial-maximum vegetation geography of the northern continents and Africa. J. Biogeogr. 27, 507–519.
Ray, N., Adams, J.M., 2001. A GIS-based vegetation map of the World at the Last Glacial Maximum (25,000–15,000 BP). Int. Archaeol. 11.
Snowball, I., Korhola, A., Briffa, K.R., Koç, N., 2004. Holocene climate dynamics in Fennoscandia and the North Atlantic. In: Battarbee, R.W., Gasse, F., Stickley, C.E. (Eds.), Past Climate Variability through Europe and Africa. Developments in Paleoenvironmental Research, vol. 6. Springer, Dordrecht, pp. 364–397.
Sugita, S., 1993. A model of pollen source area for an entire lake surface. Quat. Res. 39, 239–244.
Sugita, S., 2007a. Theory of quantitative reconstruction of vegetation I: pollen from large sites reveals regional vegetation composition. Holocene 17, 229–241.
Sugita, S., 2007b. Theory of quantitative reconstruction of vegetation II: all you need is LOVE. Holocene 17, 243–257.
Tarasov, P.E., Kremenetskii, K.V., 1995. Geochronology and stratigraphy of the Holocene lacustrine-bog deposits in northern and central Kazakhstan. Stratigr. Geol. Correl. 3, 73–80.
Tarasov, P.E., Pushenko, M.Ya., Harrison, S.P., Saarse, L., Andreev, A.A., Aleshinskaya, Z.V., Davydova, N.N., Dorofeyuk, N.I., Efremov, Yu. V., Elina, G.A., Elovicheva, Ya.K., Filimonova, L.V., Gunova, V.S., Khomutova, V.I., Kvavadze, E.V., Neustrueva, I.Yu., Pisareva, V.V., Sevastyanov, D.V., Shelekhova, T.S., Subetto, D.A., Uspenskaya, O.N., Zernitskaya, V.P., 1996. Lake status records from the Former Soviet Union and Mongolia: documentation of the second version of the data base. NOAA Paleoclimatology Publications Series Report No. 5. World Data Center A - Paleoclimatology, Boulder, 224 pp.
Tarasov, P.E., Webb III, T., Andreev, A.A., Afanas'eva, N.B., Berezina, N.A., Bezusko, L.G., Blyakharchuk, T.A., Bolikhovskaya, N.S., Cheddadi, R., Chernavskaya, M.M., Chernova, G.M., Dorofeyuk, N.I., Dirksen, V.G., Elina, G.A., Filimonova, L.V., Glebov, F.Z., Guiot, J., Gunova, V.S., Harrison, S.P., Jolly, D., Khomutova, V.I., Kvavadze, E.V., Osipova, I.M., Panova, N.K., Prentice, I.C., Saarse, L., Sevastyanov, D.V., Volkova, V.S., Zernitskaya, V.P.,

1998. Present-day and mid-Holocene biomes reconstructed from pollen and plant macrofossil data from the former Soviet Union and Mongolia. J. Biogeogr. 25, 1029–1053.

Tarasov, P.E., Peyron, O., Guiot, J., Brewer, S., Volkova, V.S., Bezusko, L.G., Dorofeyuk, N.I., Kvavadze, E.V., Osipova, I.M., Panova, N.K., 1999. Last Glacial Maximum climate of the Former Soviet Union and Mongolia reconstructed from pollen and plant macrofossil data. Clim. Dyn. 15, 227–240.

Tarasov, P.E., Volkova, V.S., Webb III, T., Guiot, J., Andreev, A.A., Bezusko, L.G., Bezusko, T.V., Bykova, G.V., Dorofeyuk, N.I., Kvavadze, E.V., Osipova, I.M., Panova, N.K., Sevastyanov, D.V., 2000. Last Glacial Maximum biomes reconstructed from pollen and plant macrofossil data from Northern Eurasia. J. Biogeogr. 27 (3), 609–620.

Tarasov, P., Granoszewski, W., Bezrukova, E., Brewer, S., Nita, M., Abzaeva, A., Oberhänsli, H., 2005. Quantitative reconstruction of the Last Interglacial vegetation and climate based on the pollen record from Lake Baikal, Russia. Clim. Dyn. 25 (6), 625–637.

Vasil'ev, S.A., Kuzmin, Y.V., Orlova, L.A., Dementiev, V.N., 2002. Radiocarbon-based chronology of the Paleolithic in Siberia and its relevance to the peopling of the New World. Radiocarbon 44 (2), 503–530.

Velichko, A.A., Wright Jr., H.E., Barnosky, C.W., 1984. Late Quaternary environments of the Soviet Union. University of Minnesota Press, Minneapolis, MN. 327 pp.

Vostokova, E.A., Gunin, P.D. (Eds.), 2005. Ecosystems of Mongolia, Atlas. Russian Academy of Sciences, Moscow. 48 pp.

Wang, Y., Cheng, H., Edwards, R.L., He, Y., Kong, X., An, Z., Wu, J., Kelly, M.J., Dykoski, C.A., Li, X., 2005. The Holocene Asian monsoon: links to solar changes and North Atlantic climate. Science 308, 854–857.

Williams, J.W., 2003. Variations in tree cover in North America since the last glacial maximum. Glob. Planet. Change 35, 1–23.

Williams, J.W., Jackson, S.T., 2003. Palynological and AVHRR observations of modern vegetational gradients in eastern North America. Holocene 13 (4), 485–497.

Williams, J.W., Shuman, B.N., Webb III, T., Bartlein, P.J., Leduc, P.L., 2004. Late Quaternary vegetation dynamics in North America: scaling from taxa to biomes. Ecol. Monogr. 74, 309–334.

Williams, J.W., Gonzales, L.M., Kaplan, J.O., in press. Leaf area index for northern and eastern North America at the Last Glacial Maximum: a data–model comparison. Glob. Ecol. Biogeogr., doi:10.1111/j.1466-8238.2007.00349.x.

Wright Jr., H.E., Kutzbach, J.E., Webb III T., Ruddiman, W.F., Street-Perrott, F.A., Bartlein, P.J. (Eds.), 1993. Global climates since the last glacial maximum. University of Minnesota Press, Minneapolis. 569 pp.